79-4038

Formation of a Trailing Vortex

Michael S. Francis*
U.S. Air Force Academy, Colo.
and
Donald A. Kennedy †
University of Colorado, Boulder, Colo.

The incompressible flowfield in the vicinity of a lifting rectangular finite wing is investigated experimentally to ascertain the nature and detailed characterisitics of the formation of a trailing vortex. The mean velocity field was mapped directly using a linearized constant temperature hot-wire anemometry probe in conjunction with a precision wind-tunnel traversing mechanism. The associated vorticity field was inferred from these measurements through a spatial contour integration procedure. The existence of several identifiable flow regions exhibiting similar characteristics was established and verified with both hot-wire and flow visualization data. The nature of the near surface bound vorticity distribution is described including a map of the Prandtl-bound vortex filaments. Measurements at the wing trailing edge show that the properly nondimensionalized characteristic vorticity distribution in this region is independent of angle of attack. Shed vorticity emanating from the lower aerodynamic surface near the wing tip was observed to roll up adjacent to the tip and roll over onto the upper wing surface at a chordwise location which depends on the wing orientation. The presence and behavior of this structure which possesses an identifiable core is suggested as the cause of the modified pressure distribution (lift increment) normally observed in this region.

Nomenclature

A = area, usually referring to that enclosed by a contour
b = wing semispan, geometric
c = wing chord length, geometric; or symbol for contour
c_l = wing section lift coefficient
l = path distance along a contour, c
p = pressure
t = local value of wing thickness
U = general symbol for velocity, subscripted to denote specific spatial components (U_x, U_y, U_z)
U_0 = freestream tunnel velocity
x = flow direction parallel to freestream
y = flow direction perpendicular to freestream extending spanwise along the wing
z = flow direction perpendicular to freestream extending normal to xy plane
Γ_c = circulation about a contour, c (subscript denotes specific contour)
Γ_0 = circulation of a contour enveloping the wing plus boundary layer at the centerline spanwise location
Δ = used as a prefix to another symbol, it implies the difference in two values of that quantity, e.g., to reflect the difference between values on the upper and lower surfaces for the same chordwise and spanwise locations
δ_u = boundary-layer thickness on upper surface
δ_l = boundary-layer thickness on lower surface
ξ = vorticity vector, $\xi = \xi_x\hat{i} + \xi_y\hat{j} + \xi_z\hat{k}$
ρ = density of fluid medium

Introduction

THIS investigation is concerned with the formation and early development of a trailing vortex resulting from lift generation on a finite wing. The process is examined experimentally, employing measurements of the velocity and vorticity fields adjacent to and immediately downstream of a rectangular wing immersed in a uniform stream. The experiments were conducted in a subsonic wind tunnel and involve nominally unseparated flow conditions over the lifting surface.

The significance of the problem can be understood more clearly by considering the entire flowfield which results from the passage of fluid over a lifting surface. Disturbances resulting from the wing's presence lead to the appearance of a wake which persists for a long time period (far downstream of the wing) and which evolves through several identifiable stages. The flow near the solid surface is classically termed the boundary layer—that region which is the source of all vorticity generated in the flowfield. The behavior of the flow in this region together with the neighboring external flow is directly related to the surface load distribution and is the primary arena of interest in this study.

The sector immediately downstream of the wing, referred to as the near wake or rollup region, is usually strongly three dimensional. Vortex filaments shed into this area are free to interact with each other, resulting in the ultimate development of two discrete vortices of opposing rotation. A number of investigators have studied the motion of these vortices including their stability, their interaction under various environmental conditions, and their decay. Prediction methods for their interaction with encountering aircraft have also been developed. They have been studied theoretically, numerically, and experimentally in both laboratory experiments and in flight tests. In short, many aspects of the flow in the wake region are reasonably well documented.

This is not the case, however, with the flow in the immediate vicinity of the wing. The qualitative nature of the flow was first sketched by Lanchester[1] and later visualized by Hoerner.[2] Driven by the need for aircraft design data, early experimental efforts concentrated largely on the measurements of integral effects (e.g., lift coefficient) and the surface pressure distribution, with little emphasis on related flowfield effects. In a very few instances, attempts were made to relate these effects to the surface load characteristics.[3] The current focus on the problem of wake vortex alleviation has re-emphasized the need for an accurate assessment of the flow

Received April 5, 1978; revision received Aug. 17, 1978.

Index category: Aerodynamics.

*Capt, USAF, Chief, Mechanics Division, Frank J. Seiler Research Laboratory. Member AIAA.

†Assistant Professor, Dept. of Aerospace Engineering Sciences. Member AIAA.

conditions in the immediate vicinity of the generator.[4] A few experiments have addressed this question but have been limited to the measurement of specific characteristics in that part of the tip region exhibiting an identifiable vortex geometry.[5]

Recent computational efforts to predict the flowfield behavior based on vorticity field structure are hampered by the necessity for user supplied initial conditions and assumptions which model vortex sheet transition from the bound to the free state.[6-8] An additional shortcoming in these analyses is the treatment of flow behavior near the tip. In many situations, a resulting mathematical singularity in the vorticity distribution which corresponds to a locally infinite value of velocity must be resolved using techniques which artificially remove or ignore the singularity.[9]

The actual physical situation is related to the analytical model through the concept of bound vorticity. In potential theory, this entity is usually ascribed to the body in contrast with free vorticity which remains with the fluid elements. In reality, the bound vorticity is actually that which is continually generated by shear in the wing boundary layer and which appears attached to the wing in the Eulerian reference frame. In two-dimensional flow or at the symmetry plane of a finite wing, the vorticity vector is perpendicular to the freestream direction.

Of equal significance is the apparent redirection of vorticity toward the freestream direction, e.g., the horseshoe vortex concept. The actual reorientation of vorticity is caused by the spanwise variation of the pressure gradient over the surface. If one considers the effects on a fluid element which lies near the surface, it is observed to deform and rotate due to the influence of the crossflow velocity gradient as well as that in the mainflow direction. As it moves within the boundary layer, it continues to be affected by this rotational tendency depending, of course, on the strength and character of the crossflow shear. Eventually, the element enters the free field at some point of boundary-layer separation (trailing edge, wing tip, or other location where the layer separates) where it becomes part of a free vortex filament in the wake. The preceding description is not strictly accurate since the hypothetical element is, of course, distorted and diffused as it moves over even a small distance, but the concept serves a pedagogical purpose in describing the origins of mainstream-directed vorticity. This simplistic view is also complicated by the presence of free vorticity near the surface which is not accounted for in the sheet models employed to describe most wings.

Description of the Experiment

The determination of the flowfield around a semispan, wall-mounted, finite wing model involved both hot-wire anemometry and flow visualization techniques. The hot-wire measurements were conducted in the University of Colorado 61-cm × 61-cm (2-ft × 2-ft) low turbulence wind tunnel, while the flow visualization photographs were taken in the U.S. Air Force Academy 61-cm × 91-cm (2-ft × 3-ft) subsonic wind tunnel. The same wing model was employed in both sets of measurements.

The selection of a suitable lifting shape for the experiment was predicated on both aerodynamic considerations and facility limitations. A simple geometry having a thin cross section seemed desirable in order to simplify the theoretical aspects of the problem. An airfoil shape which reasonably satisfied the conditions of thin airfoil theory while yielding minimal wake and boundary-layer displacement characteristics was required to physically emulate the simple, potential flow theoretical models. Since the detailed flowfield about the wing was to be investigated, considerations of the position resolution capabilities of the apparatus and the minimum effective probe size demanded a comparatively large wing chord. The relatively small tunnel cross section, however, imposed a severe restriction on the span parameter, thus limiting the maximum effective aspect ratio.

On these bases a rectangular, untwisted wing having a NACA 64009 airfoil cross section was constructed with a 20.3-cm (8-in.) chord and 30.5-cm (12-in) semispan (half aspect ratio of 1.5). The wing was attached to the test section wall with a large end plate and protruded to the center of the test section. The angle of attack could be varied to within ±0.25 deg by a rotation mechanism outside the tunnel. The surface was finely polished in attempt to preserve the laminar flow characteristics and minimize boundary-layer displacement effects. To provide an accurate geometric reference for the velocity field measurements, dark black spanwise lines were drawn over the white finish on both upper and lower surfaces and extended around the exposed tip side at 5% chord increments from the leading to the trailing edge.

A linearized constant temperature hot-wire anemometer based on a design by Freymuth[10] was employed for the measurement of both mean and turbulent fluid velocities. Probe sensors were of platinum-10% rhodium composition. X-configuration hot-wire probes were used to determine orthogonal velocity components using simple operational amplifier addition and subtraction circuits. An X-wire analog processing circuit[11] was used for filtering, averaging, and integrating the velocity field signals.

The nature of the investigation demanded that the velocity field be resolved into components. Since an unseparated, surface-bounded flow was to be studied, an X-wire probe was constructed having a variable head angle where the plane of the X could be rotated to ±40 deg. Alignment of the probe so that the plane of the X was locally parallel to the model surface effectively provided the total velocity vector in most measurement regions. Standard fixed angle X-meters were also employed for flowfield measurements at distances further away from the model.

A precision traversing mechanism was constructed to provide accurate positioning of the measuring probes. The probe body could be moved either vertically or horizontally (xy plane) with a drive provided by miniature dc motors. Geared precision potentiometers were utilized to monitor distances in both of these directions. A Gaertner optical cathetometer was used to establish reference distances between the model and the probes in various configurations. Utilizing this device, probes could be positioned to within 1.27 mm of the model surface without establishing physical contact. Most of the measurements were conducted at a freestream tunnel velocity of 18.3 m/s (60 fps), the maximum speed for which probe vibration effects were negligible. The corresponding Reynolds number based on wing chord was 247,000.

The measurement of vorticity in the flow was accomplished using the definition of circulation as follows

$$\Gamma_c = \oint_c \boldsymbol{U}\cdot \mathrm{d}\boldsymbol{l} = \int\int_A \boldsymbol{\xi}\cdot \mathrm{d}\boldsymbol{A} \tag{1}$$

For a planar contour c oriented normal to the x direction, this can be written as

$$\langle \xi_x \rangle = \frac{1}{A}\oint_c \boldsymbol{U}\cdot \mathrm{d}\boldsymbol{l} \tag{2}$$

where the brackets denote a spatial average. Contour integral paths were traced out in physical space by the probe traversing mechanism. The restriction to independent horizontal or vertical movement restricted these curves to being rectangles in the crossflow plane. By orienting the probe such that the x plane was parallel to the traversal direction, the quantities appearing in Eqs. (1) and (2) were evaluated. The restrictions and limitations of using this technique with an X-wire probe in a three-dimensional flow have been discussed by Francis and Kennedy.[12]

This technique can also be employed in the vicinity of solid boundaries to measure bound vorticity. Consider a rectangular contour c enveloping the cross section of a lifting

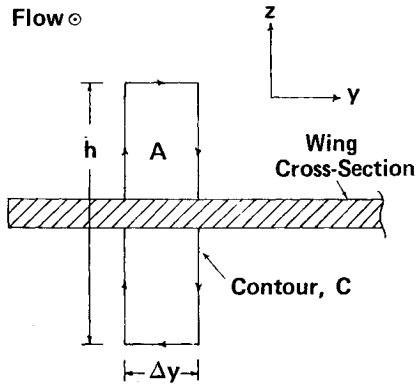

Fig. 1 Contour integration adjacent to the wing surface.

wing as shown in Fig. 1. Furthermore, let the y-direction segments of the contour lie completely outside the upper and lower surface boundary layers. The circulation about this region can be expressed

$$\Gamma_c = \oint_c U \cdot dl = \int_{-h/2}^{h/2} \left[U_z(y+\Delta y, z') - U_z(y, z') \right] dz' + \int_{y}^{y+\Delta y} \left[U_y\left(y', -\frac{h}{2}\right) - U_y\left(y', \frac{h}{2}\right) \right] dy' \tag{3}$$

From Stokes' theorem, this integral is also related to the vorticity as follows

$$\Gamma = \int\int_A \xi \cdot dA = \int_{-h/2}^{h/2} \int_{y}^{y+\Delta y} \xi_x \, dy' \, dz' \tag{4}$$

By equating these expressions and taking the limit as Δy approaches zero, the following equation is obtained:

$$\int_{-h/2}^{h/2} \xi_x \, dz' = \Delta U_y(y) \tag{5}$$

where

$$\Delta U_y(y) \equiv U_y(y, -h/2) - U_y(y, h/2)$$

Expressed in terms of an average in the z direction

$$\langle \xi_z(y;h) \rangle = [\Delta U_y(y)]/h \tag{6}$$

Hence, a direct relationship between the boundary-layer vorticity and the surface crossflow differential has been established. If the wing and boundary-layer thicknesses are negligibly thin ($h \to 0$, a vortex sheet), the crossflow differential defines the strength of the sheet. The reasons for the selection of a thin wing with a small displacement region are thus apparent. A graph of ΔU_y as a function of spanwise position will then give the shape of the vorticity distribution when $\Delta z = h$ is kept constant. The utilization of this technique to measure vorticity close to the surface should then give accurate results over the inboard portions of the wing as shown later. Its applicability is predicated on the assumption that the wing plus boundary-layer regions exhibit a sheetlike geometry of finite thickness, $h = \text{Order}(t + \delta_u + \delta_l)$.

Supportive flow visualization photographs were obtained using scattered light from tiny helium-filled, neutrally buoyant soap bubbles injected into the freestream at approximately the freestream velocity. The bubbles were provided by a Sage Action, Inc., bubble generator located in the plenum chamber of the U.S. Air Force Academy subsonic wind tunnel. The visualization results were used to confirm the qualitative aspects of flowfield behavior inferred from hot-wire results and to provide an additional source for the estimation of X-probe data errors.

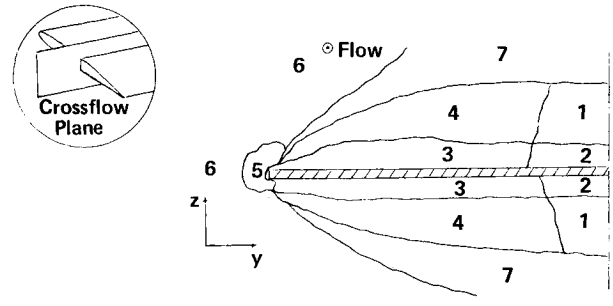

Fig. 2 Flow regions in the crossflow plane.

General Description of the Flow

An examination of the behavior of the flowfield in any crossflow plane intersecting the wing surface reveals a general structure which is qualitatively independent of the chordwise location. A sketch detailing this structure is shown in Fig. 2. The flow is subdivided into various sections which exhibit similar properties. The relative physical sizes of these regions will vary with chord location and other aerodynamic parameters (e.g., angle of attack). The advantage of this subdivision concept is that it facilitates the description and analysis within any given region. While this particular description has evolved from an investigation of a specific rectangular wing shape, the result can be generalized to a broader class of planforms, aspect ratios, and angles of attack providing the flow is unseparated in the inboard regions.

The simplest region from an analytical standpoint is that of two-dimensional (airfoil) potential flow inboard of the wing tip and outside the boundary layers on both surfaces (Region 1). It can be located about most constant chord, unswept wings of high aspect ratio, but more frequently is realized only in the wing symmetry plane as is the case in this experiment. An adjacent two-dimensional boundary layer (Region 2) can also be present. This airfoil-like flowfield coincides with the flattening of the spanwise lift distribution near the wing centerline.

The three-dimensional wing boundary layer (Region 3) is a complex structure whose velocity field is a function of all spatial variables. It is this region that is solely responsible for the generation of vorticity in the main flow direction. The local upper surface boundary-layer thickness was observed to be a strong function of chordwise location but almost independent of spanwise position except in the immediate vicinity of the tip. The weak spanwise variation was probably due to irregularities in wing thickness and surface roughness related to construction tolerances. The layer thickness varied from immeasurably thin upstream of the midwing point to over 76 mm near the trailing edge. Measurements of U_z/U_∞ near the surface were used to verify that the measured value of the downwash coincided with the calculated value of the local surface slope. The absence of separation was confirmed by these measurements over the angle-of-attack range of 0-8 deg.

A region of considerable interest is that of three-dimensional potential flow just outside the boundary layer and inboard of the tip (Region 4 in Fig. 2). It is this sector that will be involved in the computation of wing bound vorticity later. Examination of the crossflow variation reveals that it is apparently not dependent on the normal (z) coordinate in this region. This important simplification is readily understood by examining the equation for the x-vorticity component:

$$\xi_x = \frac{\partial U_z}{\partial y} - \frac{\partial U_y}{\partial z} \tag{7}$$

The left side of this expression is zero since only potential flow is considered. Since for the untwisted, nonporous wing with a

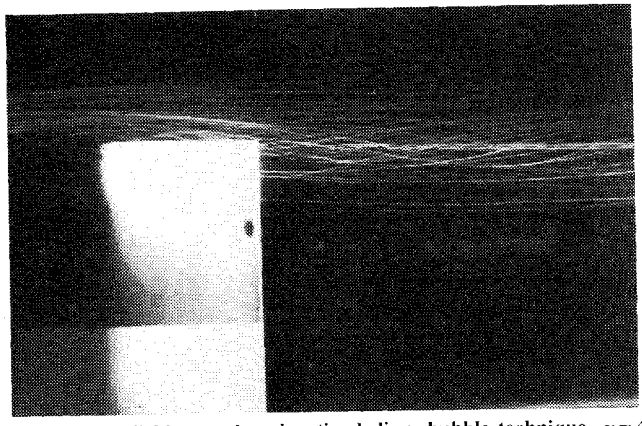

Fig. 3 Flowfield near the wing tip, helium bubble technique, $\alpha = 4$ deg, $U_0 = 18.3$ m/s.

thin uniform boundary layer the streamlines approximately follow the surface contour, then

$$\frac{\partial U_z}{\partial y} \approx 0$$

and the preceding equation reduces to

$$\frac{\partial U_y}{\partial z} = 0 \qquad U_y = U_y(x,y) \text{ only} \tag{8}$$

This equation is verified by the existing experimental evidence. The approximation breaks down several boundary-layer thicknesses away from the surface due to the influence of other elements of the flowfield. The simplification does, however, allow a wide margin for error in the measurement location employed for calculating the bound vorticity. The wing orientation and thin boundary-layer geometry greatly contributed to the accuracy of the approximation in this case.

The flow immediately adjacent to the wing tip is characterized by the presence of steep velocity gradients over a small spatial region in addition to an irregular geometric structure. In contrast to its regular behavior in the inboard region, the crossflow near the tip is observed to be highly dependent on all spatial coordinates. This area, represented by Region 5 of Fig. 2, is one characterized by concentrated vorticity which has accumulated due to shedding upstream in the tip region. The helical flow pattern so commonly associated with the far-field isolated vortices is observed to develop well upstream of the trailing edge as can be seen in the streak photograph in Fig. 3. Further examination shows this lump of vorticity adheres to both the sides and upper surface of the tip region.

The actual identity of this region is doubtlessly related to the wing tip shape in addition to other wing parameters. The measurements described here concern only a flat tip whose plane is perpendicular to the y coordinate. Since the tip is frequently the source of a singularity in theoretical or numerical analyses, the physical characteristics of this portion of the flowfield are significant.

The approximate shape of this rollup region in various crossflow-plane stations along the wing has been reconstructed using detailed X-wire data. Horizontal and vertical traverses at finely spaced intervals were used to construct crossflow plane velocity vectors, local maxima and minima, and crossflow stagnation points, lines, and regions. A small portion of this reconstruction is displayed in Fig. 4. An examination of these results initially suggests the possibility of prohibitively large measurement errors due to the presence of strong rotational gradients. In fact, the large values of the corresponding freestream-oriented velocity component provide sufficient bias to reduce the values of local flow angle (less than 22 deg) to within the limits of X-probe operation. Typical errors encountered in assessing the crossflow velocity component were estimated at 2-4%. The worst-case local error detected in these measurements occurred in the crossflow reconstruction at the 50% chord location (not shown). It was estimated to be as high as approximately 12% at one location.

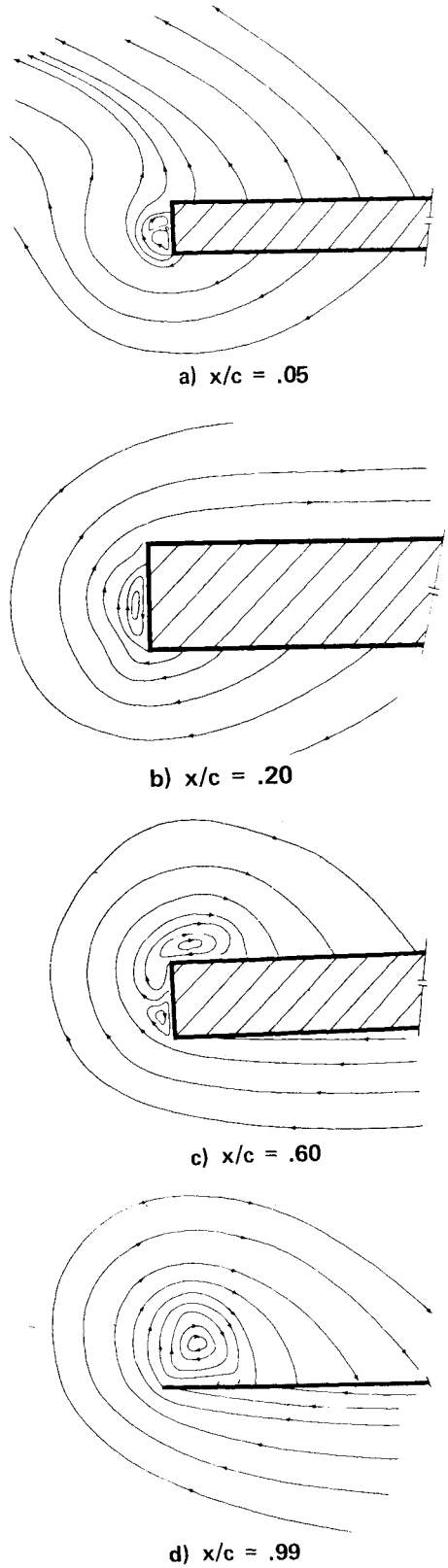

Fig. 4 Projection of streamlines in the crossflow plane, wing tip region, $\alpha = 4$ deg, $U_0 = 18.3$ m/s.

The swirling secondary flow is observed to originate close to the leading edge (first detected at $x/c = 0.05$) and progress aft along the side of the wing. Its growth is restricted to the

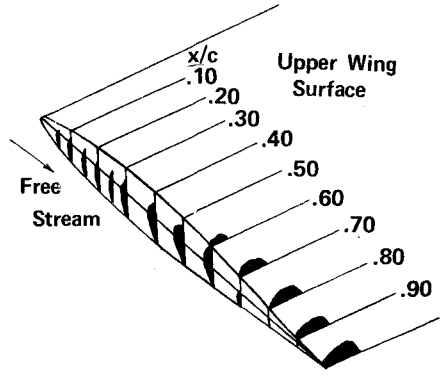

Fig. 5 Regions of "reverse crossflow," wing tip region, $\alpha = 4$ deg, $U_0 = 18.3$ m/s.

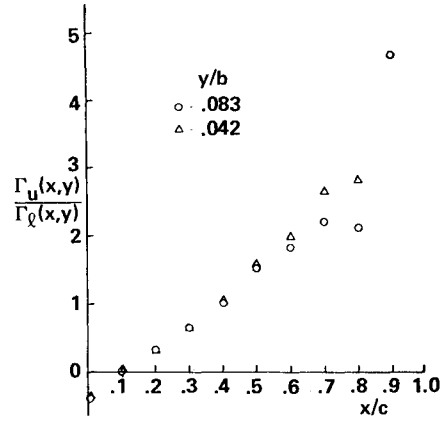

Fig. 6 Ratio of circulation functions near the tip on the upper surface to corresponding region on the lower surface, $\alpha = 4$ deg, $U_0 = 18.3$ m/s.

side portion of the tip until some location (the 60% chord point at $\alpha = 4$ deg, the condition for maximum lift-to-drag ratio) where it begins to roll over onto the upper surface. This repositioning movement is caused by the general influence of the pressure gradient around the tip. By the time the structure has reached the vicinity of the trailing edge, it is positioned almost entirely above the upper surface. The complex structure of the secondary flow at various intermediate chordwise locations is caused by the local wing tip geometry.

Figure 5 illustrates more effectively the regions where reversed crossflow exists, i.e., regions where the local crossflow direction opposes that of the nominal outer flow pressure gradient. A line representing locations of zero upwash (i.e., z-velocity component) is observed to lie almost parallel with the freestream extending rearward from the leading-edge stagnation point. These results are consistent with those of Chigier and Corsiglia[5] who measured vortex properties at several chordwise stations above the surface of an untwisted, rectangular wing at high angle of attack ($\alpha = 12$ deg). In that case, the origin of residence of the vortex over the upper surface was observed to occur upstream of the quarter-chord point. In the case of a rectangular wing, then, it may be possible to approximate the location of upper-surface tip edge separation by the intersection of a straight line drawn parallel to the freestream direction from the leading-edge stagnation point along the wing profile with the upper surface.

As might be expected, the flow surrounding this region of concentrated vorticity is dominated by its presence (induced velocity via Biot-Savart law). The streamlines in the outer region exhibit a much more well-organized spiral character approaching a cylindrical geometry as viewed in the crossflow plane (Region 6 of Fig. 2). The area denoted by Region 7 is

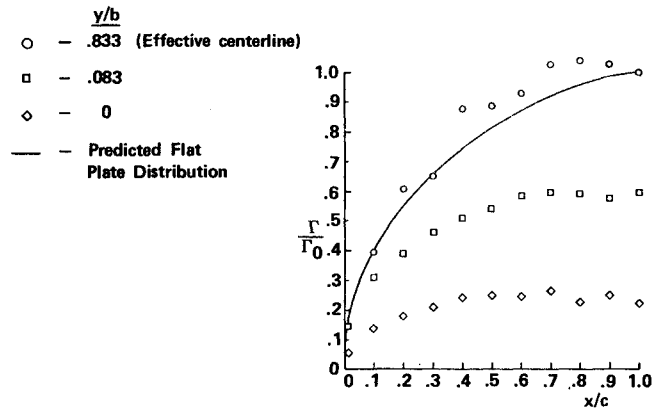

Fig. 7 Chordwise variation of wing circulation, $\alpha = 4$ deg, $U_0 = 18.3$ m/s.

one dominated equally by the concentrated tip vortex structure and the influence of the inboard surface boundary.

Vorticity Field Surrounding the Lifting Surface

A comprehensive description of the global wing vorticity field is dependent on a reconciliation of the inboard distribution which is inferred using the technique described in the preceding and the more complex rotational flow near the wing tip. Measurements of the distribution of separated vorticity in the tip region were accomplished using an array of rectangular multielement contours aligned perpendicular to the freestream direction. The contours were designed to envelop the tip region at 10% increments in chord along the surface. The distribution and size of the measurement cells were selected in an attempt to minimize measurement errors from the effects of out-of-plane flow components on the X-wire probe. By positioning the mesh geometry such that no measurement locations coincided with the vortex centroid (an iterative procedure based on previous measurments in conjunction with flow visualization photographs), pointwise measurements in regions of large curvature were minimized. The spanwise extent of the integration region was determined by the local influence of the vortex at each chordwise location.

The production of vorticity (x component) was observed to begin almost at the leading edge and predominantly on the lower wing surface. The concentration of vorticity there exceeded that adjacent to the opposing surface from the leading edge downstream to the 40% chord point at the maximum lift-to-drag test condition. From there aft, the inverse relationship was observed. Figure 6 depicts this ratio as a function of chordwise location for spanwise regions extending from the tip to 1.27 cm (0.5 in.) and 2.54 cm (1 in.) inboard, respectively. The ratio, $\Gamma_{upper}/\Gamma_{lower}$, is observed to be independent of the spanwise location forward of the 60% chord location. The deviation of the two curves downstream of this point is probably due to the rollover of free vorticity onto the upper surface and its interaction with the boundary layer.

The shedding of vorticity into the region opposite to the side of the tip was also observed to occur close to the leading edge. The extent of the vorticity contained in this area is shown in Fig. 7 which depicts the percentage of circulation associated with this region compared to the overall wing value as a function of the chordwise location. The amount is observed to increase steadily from the leading edge to the 40% chord point and thereafter remain constant to the trailing edge. This observation does not imply a sudden discontinuance of the shedding process but rather that a kind of equilibrium has been established. That is, the vorticity which is shed into the side region is equal in amount to that rolling over onto the upper surface and out of this region. This figure illustrates the comparative influence of various spanwise

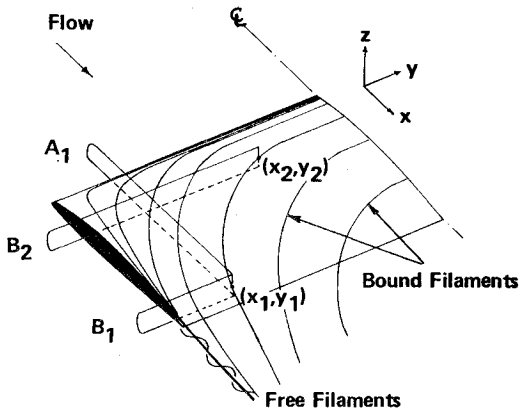

Fig. 8 Contour integrals and the bound vorticity distribution.

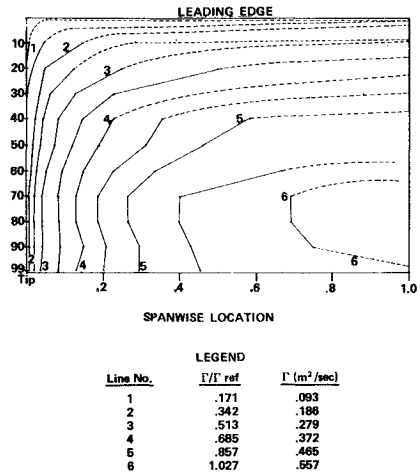

LEGEND

Line No.	Γ/Γ ref	Γ (m²/sec)
1	.171	.093
2	.342	.186
3	.513	.279
4	.685	.372
5	.857	.465
6	1.027	.557

Fig. 9 Bound vortex elements over the wing surface, $\alpha = 4$ deg, $U_0 = 18.3$ m/s.

regions on overall vorticity content. For comparison, the distribution predicted for a two-dimensional flat plate is shown.[13]

These data can now be combined with crossflow velocity differential measurements in the region inboard of the tip with the aid of the circulation function. First, consider two spanwise contours (B_1 and B_2) enveloping the wing boundary layer from outboard of the tip and extending to surface locations (x_1, y_1) and (x_2, y_2), respectively (Fig. 8). Further, assume that although these locations represent different chordwise and spanwise coordinates, the spatial circulation integral has the same value at both locations ($\Gamma_{B_1} = \Gamma_{B_2}$). If all vorticity is generated at the wing surface and passes within the contour bounds, then the same net number of equal strength vortex filaments pass between the boundaries of each contour. By connecting surface points exhibiting equal values of Γ_B, families of curves are obtained which represent lines of constant vorticity, or the traditional bound vortex lines. It must be emphasized that this description is only valid where the sheet concept can be applied, i.e., interior to the interactive flow region near the tip, though the tip region must be included in the integrals.

Figure 9 is a planform map of the bound vortex lines developed for the wing at 4-deg angle of attack. The parameter h from Eq. (6), which was used to calculate the vorticity distribution in the region inboard of the tip, was adjusted to correspond with the maximum observed value

$$h = (t + \delta_u + \delta_l)_{\max.} \tag{9}$$

Note that the general shape of the array of lines is qualitatively similar to that hypothesized in lifting line theory.

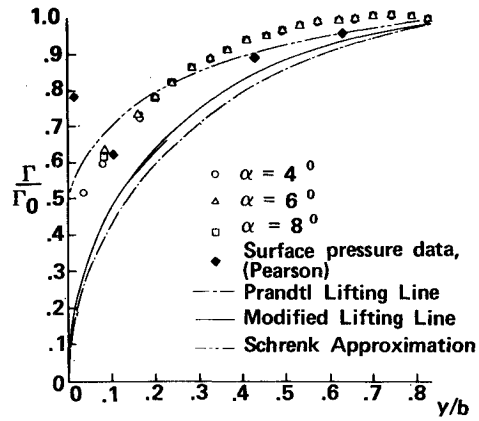

Fig. 10 Circulation function at the trailing edge, $U_0 = 18.3$ m/s.

A close examination of the figure reveals an unusual behavior near the trailing edge and wing centerline. This apparent redirection of the bound vortex lines in the spanwise direction is due to a reversal in polarity of the crossflow differential in the wall region, but not at the wing centerline as one would expect for a semispan model. This behavior is attributed to the interaction of the tunnel wall boundary layer with the wall-bound tip vortex. The net result is a reduction in the effective aspect ratio, though in a highly irregular manner. These considerations were included in the following calculation of the lift distribution.

Wing Lift Distribution

A relationship between the crossflow velocity differential, bound vorticity, and circulation was established earlier. These quantities are, in turn, related to the pressure field and, hence, the section and overall lift coefficients.

If the Kutta-Joukowski condition is imposed on the velocity at the sharp trailing edge, the lift per unit span is known to be $\rho U_0 \Gamma$, where Γ is the circulation around a circuit encompassing the wing chord and boundary layer and parallel to the freestream. The selection of this contour in an actual viscous flow is sensitive to a number of parameters, especially the location of the region of intersection of the contour with the wake. Thwaites,[13] (pp. 192-194) indicates that the error in the selection of this location is negligible providing the wing lift-drag ratio is large.

If this is the case, the section lift coefficient can be computed as

$$c_l(y) = \frac{2\Gamma_A(y)}{U_0 c} \tag{10}$$

where the A subscript refers to a chordwise oriented contour extended from the leading to trailing edges which completely encompasses all bound vorticity (Fig. 8). If it is further assumed that the wing is uniformly thin and at a small angle of attack, the following approximation can be written

$$\Gamma_A(y) \cong \int_0^c \Delta U_v(x', y)\,dx' + I_{\text{stag}}(y) + I_{\text{vis}}(y) \tag{11}$$

where I_{stag} represents the contribution to the overall contour integral in the vicinity of the leading edge (stagnation line) and I_{vis} relates the contribution due to the viscous wake near the trailing edge.

An additional relationship can be established by considering the related B contour. Conservation of vorticity requires that all of the bound vortex lines passing through the capping surface of A also pass through B. Then,

$$\Gamma_A = \Gamma_B \tag{12}$$

Due to the equivalence in the A- and B-type integrals, one can deduce

$$\Gamma_A(y) = \frac{1}{\rho U_0}\int_0^c \Delta p(x',y)\,dx' = \Gamma_B(c,y) \tag{13}$$

Similarly, the circulation function for the B-type contour can be related to the crossflow velocity differential through an extension of Eq. (3)

$$\Gamma_B(c,y) = \Gamma_{tip} + \int_{y_0}^{y} \Delta U_y(c,y')\,dy' \tag{14}$$

and, therefore,

$$\frac{\partial \Gamma(y)}{\partial y} = \Delta U_y(c,y) \tag{15}$$

where Γ_{tip} represents the overall contribution to circulation in the tip region where high rotational gradients are present. The trailing-edge circulation distribution then effectively describes the spanwise loading—at least over the inboard portions of the wing.

The measured results are displayed in Fig. 10 and are compared with modified lifting line theory,[14] the classic Shrenk approximation,[15] and Prandtl lifting line theory (elliptic lift distribution). Several data points obtained in early measurements of the surface pressure differential are also shown.[16] The pressure data and circulation measurements are seen to agree in all but the immediate vicinity of the tip, as expected. Only the Shrenk approximation appears to adequately approximate the correct behavior of the vorticity distribution. Again, however, large errors persist in the tip zone.

The repeatibility of the data for various wing orientations strongly suggests that the bound vorticity distribution is independent of angle of attack over the inboard region at least for conditions of nominally unseparated flow. Therefore, the flow picture presented in Fig. 9 is expected to apply to other values of α for which the inboard flow remains unseparated.

Care must be exercised in extending the similarity of the resulting pressure distributions with respect to angle of attack, however, especially in the vicinity of the wing tip. Though an extensive survey of the surface flow was not made at all values of α, one would expect that vortex spillover onto the upper surface should occur farther upstream with increasing incidence. This would imply a higher value for the tip lift increment (due to interaction with the surface boundary layer) and a probable variation in the section center of pressure. This was found experimentally by Pearson[16] and recently verified in calculations by Maskew.[6] In addition, measurements of increased negative section pitching moment coefficient near the tip[16] are consistent with this hypothesis.

Conclusions

The distribution of mainstream-oriented vorticity generated by crossflow velocity gradients in the boundary layer of a lifting finite wing has been investigated and discussed. Filaments of vorticity which exit the surface layer at points of separation (e.g., the tip edge) then interact with one another resulting in a rolled-up structure whose evolution is dependent on the local tip geometry and orientation. In the present case, the rollup process was observed to originate in the tip edge region near the leading edge (upstream of the 5% chord location). Since local crossflow velocity levels adjacent to the wing surfaces might reasonably be expected to vary as the intensity of corresponding pressure gradients, the appearance of a free vortex in this region is not unexpected. The residence location of the vortex was found to transition to the upper wing surface at a chordwise location dependent on the angle of attack. The extensive rollup observed adjacent to the wing surface may be attributed, in part, to the ability of the solid boundary to sustain shear.

For nominally unseparated conditions, the dimensionless form of the vorticity distribution in the region inboard of the tip was found to be independent of wing incidence. This result suggests a limited degree of influence by the character of the rolled-up vortex at the tip. However, the inboard distribution is expected to be a function of wing aspect ratio.

A comparison of the spanwise vorticity distribution at the trailing edge with measured section lift characteristics revealed a lessening degree of correlation as the tip was approached. This deviation, which culminates in a sudden lift increment (suction peak) just inboard of the tip, is consistent with the behavior of the free vortex in that region. A thorough understanding of the influence of the concentrated tip vortex must involve a systematic investigation of tip planform and cross-section geometries and should be expanded to include the effects of wing sweepback.

Acknowledgment

This research was sponsored, in part, by the Frank J. Seiler Research Laboratory.

References

[1] von Karman, T., *Aerodynamics*, 1st ed., McGraw-Hill, New York, 1963, pp. 48-53.

[2] Hoerner, S., *Fluid Dynamic Drag*, 1st ed., Published by Author, Bricktown, N.J., 1951, Chap. VII.

[3] Bryant, L.W. and Williams, D.H., "An Investigation of the Flow of Air Around an Aerofoil of Infinite Span," Philosophical Transactions of the Royal Society, A, Vol. 225, 1925, pp. 199-237.

[4] Rossow, V.J., "Survey of Computational Methods for Lift-Generated Wakes," NASA SP-347, March 1975.

[5] Chigier, N.A. and Corsiglia, V.R., "Tip Vortices—Velocity Distributions," NASA TM X-62,087, Sept. 1971.

[6] Maskew, B., "A Quadrilateral Vortex Method Applied to Configurations with High Circulation," NASA SP-405, May 1976.

[7] Kandil, O.A., Mook, D.T., and Nayfeh, A.H., "Nonlinear Prediction of the Aerodynamic Loads on Lifting Surfaces," AIAA Paper 74-503, *Journal of Aircraft*, Jan. 1976, pp. 22-28.

[8] Rom, J., Zorea, C., and Gordon, R., "On the Calculation of Non-linear Aerodynamic Characteristics and the Near Vortex Wake," Ninth Congress of the International Council of The Aeronautical Sciences, Paper No. 74-27, Haifa, Israel, Aug. 25-30, 1974.

[9] Jordan, P.F., "The Parabolic Wing Tip in Subsonic Flow," AIAA Paper 71-10, New York, N.Y., Jan. 25-27, 1971.

[10] Freymuth, P., "Feedback Control Theory for Constant-Temperature Hot-Wire Anemometers," *The Review of Scientific Instruments*, Vol. 38, May 1967, pp. 677-681.

[11] McMichael, J.M., "A Study of the Axisymmetric Turbulent Wake Generated by Co-Flowing Incompressible Streams," Ph.D. Thesis, Aerospace Engineering Sciences, University of Colorado, Boulder, Colo., 1971.

[12] Francis, M.S., Kennedy, D.A., and Butler, G.A., "A Technique for the Measurement of Spatial Vorticity Distribution," *Review of Scientific Instruments*, Vol. 49, May 1978, pp. 617-623.

[13] Thwaites, B. (ed.), *Incompressible Aerodynamics*, Oxford, Clarendon, 1960.

[14] DeYoung, J. and Harper, C.W., "Theoretical Symmetric Span Loading at Subsonic Speeds for Wings Having Arbitrary Plan Form," NACA Tech. Rept. No. 921, 1950.

[15] Schrenk, O., "A Simple Approximation Method for Obtaining the Spanwise Lift Distribution," NACA Tech. Memo.No. 948, Aug. 1940.

[16] Pearson, H.A., "Empirical Corrections to the Span Load Distribution at the Tip," NACA Tech. Note 606, 1937.